Journal of Physiology (1993), **466**, *pp.* 329–344
With 7 figures
Printed in Great Britain

PROTON CURRENTS IN HUMAN GRANULOCYTES: REGULATION BY MEMBRANE POTENTIAL AND INTRACELLULAR pH

BY NICOLAS DEMAUREX*†, SERGIO GRINSTEIN‡, MARISA JACONI*, WERNER SCHLEGEL*, DANIEL P. LEW* AND KARL-HEINZ KRAUSE*

*From the *Infectious Diseases Division, University Hospital Geneva and Fondation pour Recherches Médicales, 1211 Geneva 4, Switzerland and the ‡Division of Cell Biology, the Hospital for Sick Children, 555 University Avenue, Toronto, ON M5G 1X8, Canada*

(*Received 9 October 1992*)

SUMMARY

1. To determine whether conductive pathways contribute to the H^+ efflux from granulocytes, we used the whole-cell patch-clamp technique combined with microfluorimetric determinations of cytosolic pH (pH_i) in single, dimethylsulphoxide-differentiated HL-60 cells.

2. In voltage-clamp mode, depolarization of the cell from the resting potential (around −60 mV) to +60 mV caused an increase in pH_i that was accompanied by a sizeable outward current.

3. Ion substitution experiments and analysis of the reversal potential of tail currents indicated that the outward current is carried largely by H^+ ions.

4. Full activation of the H^+ current occurred within 1–2 s after depolarization and deactivation within 100–200 ms upon repolarization.

5. This H^+ conductance was strongly dependent on pH_i, being larger at acidic pH. In addition, at low pH_i the threshold for voltage activation of the H^+ conductance was shifted to more negative values.

6. Addition of millimolar concentrations of Cd^{2+} and Zn^{2+} to the bath solution reduced the maximum H^+ conductance and shifted the voltage dependence of the H^+ conductance to more positive potentials. The effects were reversible.

7. In conclusion, our results demonstrate that granulocytic HL-60 cells possess a voltage-gated and pH_i-sensitive H^+ conductance. Because both a depolarization and a cytosolic acidification occur during the activation of granulocytes, this conductance may play a role in pH_i homeostasis of granulocytes during microbial killing.

INTRODUCTION

Stimulation of neutrophils by a variety of agents leads to the activation of a respiratory burst. This reaction involves the one-electron reduction of molecular oxygen to superoxide, catalysed by the NADPH–oxidase complex (Babior, 1978;

† To whom correspondence should be addressed.

MS 1831

Borregaard & Tauber, 1984). Superoxide and a variety of reduced oxygen metabolites generated therefrom are essential for the microbial activity of neutrophils (Sha'afi & Molski, 1988; Clark, 1990). The oxidation of NADPH is associated with an acceleration of the hexose phosphate shunt, which is limited by the availability of $NADP^+$. The simultaneous activation of the NADPH oxidase and of the hexose phosphate shunt results in a large enhancement of the rate of metabolic acid generation (Borregaard, Schwartz & Tauber, 1984; Grinstein & Furuya, 1986). Despite this increased acid production, the cytosolic pH (pH_i) remains near neutrality and can even become more alkaline during activation (Simchowitz, 1985; Grinstein, Furuya & Biggar, 1986). These findings suggest the existence of effective pathways for net H^+ extrusion. Indeed, an active Na^+–H^+ exchanger has been described in granulocytes, which is activated directly by chemoattractants and indirectly by the local accumulation of metabolic acid (Grinstein *et al.* 1986; Grinstein, Furuya & Rotstein, 1988). The presence of a vacuolar-type H^+ pump has also been suggested (Grinstein *et al.* 1988). In addition, recent studies using pH-sensitive fluorescent probes have provided indirect evidence for the existence of a H^+ conductive pathway in stimulated neutrophils (Nanda & Grinstein, 1991; Kapus, Szászi & Ligeti, 1992). Given the appropriate proton-motive force, such a pathway could conceivably contribute to the net extrusion of H^+ from activated cells.

Using conventional electrophysiological determinations and intracellular pH measurements with pH-sensitive microelectrodes, H^+ conductances were detected in snail neurons and axolotl oocytes (Thomas & Meech, 1982; Byerly, Meech & Moody, 1984; Barish & Baud, 1984). Very recently, a H^+ conductance was also described in mammalian alveolar epithelial cells, using patch pipettes (DeCoursey, 1991). In the present study we investigated whether an analogous H^+-selective conductance, capable of acid extrusion from activated cells, was present in granulocytic cells. Using the whole-cell configuration of the patch-clamp technique, in combination with fluorescence ratio determinations of pH_i, we could detect a substantial H^+ conductance in the plasma membrane of dimethylsulphoxide-differentiated (granulocytic) HL-60 cells. The H^+ currents recorded were activated by cytosolic acidification and by plasma membrane depolarization, suggesting that they may be involved in pH_i homeostasis during granulocyte stimulation.

METHODS

Materials

The composition of the buffers used in this study is shown in Table 1. All chemicals were of analytical grade and obtained from Sigma, Merck or Fluka. The pH-sensitive fluorescent dye 5′ (and 6′)-carboxy-10-dimethylamino-3-hydroxy-spiro[7H-benzo[c]xanthene-7,1′(3′H)-isobenzofuran]-3′-one (carboxy-SNARF-1, free and acetoxymethylester form) was purchased from Molecular Probes (Eugene, OR, USA).

Cell culture

HL-60 cells were cultured in RPMI 1640 medium supplemented with 10% fetal calf serum, penicillin (5 units/ml) and streptomycin (50 μg/ml). The cells were cultured at 37 °C in an incubator with an atmosphere containing 5% CO_2. The cells were replated twice weekly and differentiated by addition of dimethyl sulphoxide (final concentration 1·3% v/v) to the cell suspension 7 days before experiments.

Measurement of cytosolic pH

The dual emission pH indicator carboxy-SNARF-1 was used for measurement of pH_i in single cells (Buckler & Vaughan Jones, 1990; Bassnett, Reinisch & Beebe, 1990). Cells (2×10^7/ml) were incubated with 5 μM carboxy-SNARF-1 acetoxymethyl ester for 30 min at 37 °C. The cells were then sedimented, resuspended in a Krebs–Ringer solution and kept at room temperature until use. An aliquot of 10^6 cells was overlaid and allowed to adhere onto a glass coverslip. All experiments were performed at room temperature within 1 h after adherence. An inverted microscope (Nikon Diaphot, Nikon Corp, Tokyo, Japan) equipped with the appropriate filters (Glen Specta Ltd, Stanmore, UK) was used for measurement of carboxy-SNARF-1 fluorescence. The excitation light, provided by a mercury lamp, was first attenuated 32 times using neutral density filters, then selected by a 515 ± 10 nm interference filter and reflected onto the stage by a 540 nm dichroic mirror. A second dichroic mirror (610 nm) was used to separate the emitted fluorescence. Emitted light of < 610 nm was filtered through a 580 ± 20 nm filter, whereas light > 610 nm was selected by a 640 ± 20 nm filter. The fluorescence intensity at 580 and 640 nm was measured simultaneously on two photometers (Hammamatsu, Japan). The photometric data were recorded at a rate of 50 Hz using a 12 bit A–D converter (Acqui, Sicmu, Geneva) and stored in an AT computer.

Calibration of the fluorescence signal *vs.* pH was performed in K^+-rich medium with the K^+–H^+ ionophore nigericin, as described previously (Mariot, Sartor, Audin & Dufy, 1991).

Patch-clamp recording

Clamping in the whole-cell configuration was performed essentially as described previously (Hamill, Marty, Neher, Sakmann & Sigworth, 1981; Krause & Welsh, 1989; Demaurex, Schlegel, Varnai, Mayr, Lew & Krause, 1992). Patch pipettes were pulled from borosilicate glass using a BB-CH-PC puller (Mecanex, Nyon, Switzerland). Pipette resistance ranged between 5 and 20 MΩ and seal resistance was between 5 and 50 GΩ. Patch recordings were performed using a LIST EPC-7 amplifier (List Medical, Darmstadt, Germany) in the voltage clamp mode. Values for whole-cell resistance varied between 2·5 and 30 GΩ, mean access resistance was between 10 and 30 MΩ and was not compensated. Cell capacitance ranged from 2 to 8 pF. Voltage pulses were provided by an eight-channel stimulator (AMPI, Jerusalem, Israel). Currents were filtered at 3 kHz and data recorded at 1 ms intervals. The same A–D converter used for pH_i recording was also utilized for acquisition of electrophysiological data. Leak currents were small compared to the studied currents and were subtracted only to allow calculation of the whole-cell conductance.

When measuring current and pH_i simultaneously, 25 μM carboxy-SNARF-1 (free acid) was added to the pipette filling solution.

RESULTS

Equilibration of cytosolic and pipette pH

It is generally assumed that, when patch-clamping small cells such as HL-60 granulocytes in the whole-cell configuration, the cytosol is readily dialysed and its ionic composition equilibrates with that of the pipette filling solution. To determine whether this is also the case for H^+, we determined the effect of varying pipette composition on pH_i, measured fluorimetrically as described above. Pipette solutions were buffered at pH values ranging from 5·5 to 8·0 using high or low buffering capacity (pipette solutions (PS) I–V in Table 1). Rupturing the membrane to achieve the whole-cell configuration caused an immediate alteration of the carboxy-SNARF-1 fluorescence ratio when the pipette pH was buffered at non-physiological values (Fig. 1). A new steady-state ratio was reached within 3 min, at a level dependent not only on the pH but also on the buffering power of the pipette filling solution. Higher concentrations of buffer resulted in faster and more profound alterations in the fluorescence ratio (cf. traces labelled pH 5·5, 10 Mes and pH 5·5, 100 Mes in Fig. 1). Thus, when using high (100 mM) concentrations of buffer in the pipette solution, the

fluorimetrically measured pH_i (y-axis, Fig. 1) was close to the pipette pH (see trace labelled pH 5·5, 100 Mes, Fig. 1). The slight deviation of the measured pH from the pipette pH might be either due to slightly different fluorescence properties of carboxy-SNARF-1 in patched cells compared to intact cells, or to a small residual H^+ gradient between the pipette and the cytosol.

TABLE 1. Composition of internal and external solutions

A. Pipette solutions

PS	pH	Salt	Buffer	Acid/base
I	7·5	140 KCl	10 Hepes	5 KOH
II	6·5	140 KCl	10 Pipes	13·2 KOH
III	5·5	140 KCl	10 Mes	2 KOH
IV	8·0	140 KCl	10 Hepes	7·6 KOH
V	5·5	90 KCl	100 Mes	20 KOH
VI	5·5	90 NaCl	100 Mes	20 NaOH
VII	5·5	90 CsAsp	100 Mes	20 CsOH
VIII	6·5	35 CsAsp	100 Pipes	132 CsOH
IX	7·5	75 CsAsp	100 Hepes	50 CsOH
X	8·0	77·5 CsAsp	100 Tris	44·2 aspartic acid

B. Bath solutions

BS	pH	Salt	Buffer	Acid/base
I	7·5	140 KCl	10 Hepes	5 KOH
II	7·5	75 KCl	100 Hepes	50 KOH
III	7·5	75 NaCl	100 Hepes	50 NaOH
IV	7·5	75 CsAsp	100 Hepes	50 CsOH

For each solution used (labelled from I to X for the pipette solutions (PS) and I to IV for bath solutions (BS), column 1) are given the final pH value (column 2) and the concentration (mM) of the major ionic species (column 3), of the different pH buffer used (column 4), and of the base or acid added to set the pH of the solution to its final value (column 5). 1 mM $MgCl_2$ and 0·2 mM EGTA were added to all the solutions, and all pipette solutions contained in addition 1 mM MgATP and 25 μM carboxy-SNARF-1 free acid. For experiments with Cd^{2+}, 3 mM $CdCl_2$ was added to bath solution IV. To correct for the binding of Cd^{2+} to the different ligands (EGTA and aspartate), the concentration of free Cd^{2+} was calculated. The free Cd^{2+} concentration in a mixture containing 3 mM Cd^{2+} and 75 mM aspartate at pH 7·5 was found to be 150 μM. Hepes, *N*-[2-hydroxyethyl] piperazine-*N'*-[2-ethanesulphonic acid]; Mes, 2[*N*-morpholino]ethanesulphonic acid; Pipes, piperazine-*N*,*N'*-bis[2-ethanesulphonic acid]; Tris, tris[hydroxymethyl]aminomethane.

Effect of membrane potential on pH_i and whole-cell currents

To study the effect of the plasma membrane potential (E_m) on transmembrane H^+ fluxes, we simultaneously measured pH_i and transmembrane currents in HL-60 granulocytes patch-clamped in the whole-cell configuration. Pipette solutions with a relatively low buffering capacity (i.e. 10 mM Hepes or piperazine-*N*,*N'*-bis(2-ethanesulphonic acid) (Pipes)) were used to facilitate detection of the voltage-induced pH_i changes. As shown in Fig. 2*A*, when the pH of the pipette filling solution was 6·5, depolarization from the holding voltage of −60 mV to 0 mV did not appreciably alter pH_i over a 30 s time course. In contrast, a sizeable outward current was associated with a further depolarization to +60 mV. This current reached a maximal

level within seconds and slowly decayed thereafter. An intracellular alkalosis accompanied the outward current, as revealed by carboxy-SNARF-1 fluorescence determinations of pH_i. The rate of alkalinization reached a maximal level within seconds and then gradually decreased, mirroring the behaviour of the outward

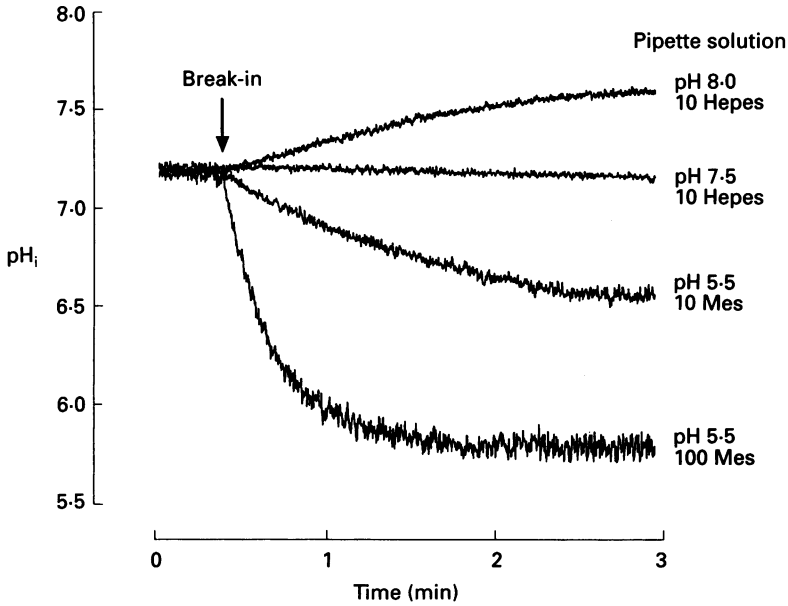

Fig. 1. Effect of pipette pH on cytosolic pH (pH_i) in whole-cell patch-clamped HL-60 cells. HL-60 cells were loaded with carboxy-SNARF-1 by incubation with the ester precursor, allowed to adhere to glass coverslips and patch-clamped. Pipette pH ranged from 5·5 to 8·0 (pipette filling solutions PS I, III, IV and V; see Table 1); bath pH was 7·5 in all experiments (solution BS I). The effect of varying pipette pH on pH_i, measured with carboxy-SNARF-1, is shown. The time at which the membrane was ruptured, achieving the whole-cell configuration, is indicated. Traces have been superimposed for comparison. Each trace is representative of 4 to 21 experiments.

current. Similar experiments were performed using a pipette pH of 7·5 (Fig. 2*B*). Under these conditions, only a minute outward current was elicited at +60 mV. Concomitantly, a modest but clearly detectable alkalinization was recorded. Together, these observations indicate that HL-60 cells possess a membrane conductance which is activated at depolarized potentials, depends on pH_i, and, when activated, is associated with changes in cytosolic pH.

Based on the cell volume and cytosolic buffering power, the H^+ fluxes necessary to support a given pH_i change can be calculated. Assuming a specific capacitance of 1 μF/cm^2 (Hille, 1992), and a spherical geometry, the 3 pF capacitance measured typically in HL-60 cells translates into a cell volume of 0·5 pl (radius 5 μm). Taking the values from Fig. 2*A* and assuming a buffering power of 28 mM of H^+ equivalents per pH unit for HL-60 cells (Grinstein & Furuya, 1986), the 1 unit increase in pH_i measured over a 30 s time course corresponds approximately to a change in intracellular [H^+] of 1 mM/s. For a cell volume of 0·5 pl this gives a value of 5×10^{-16} mol/s of H^+ leaving the cell, i.e. transmembrane H^+ fluxes of 3×10^8 ions/s.

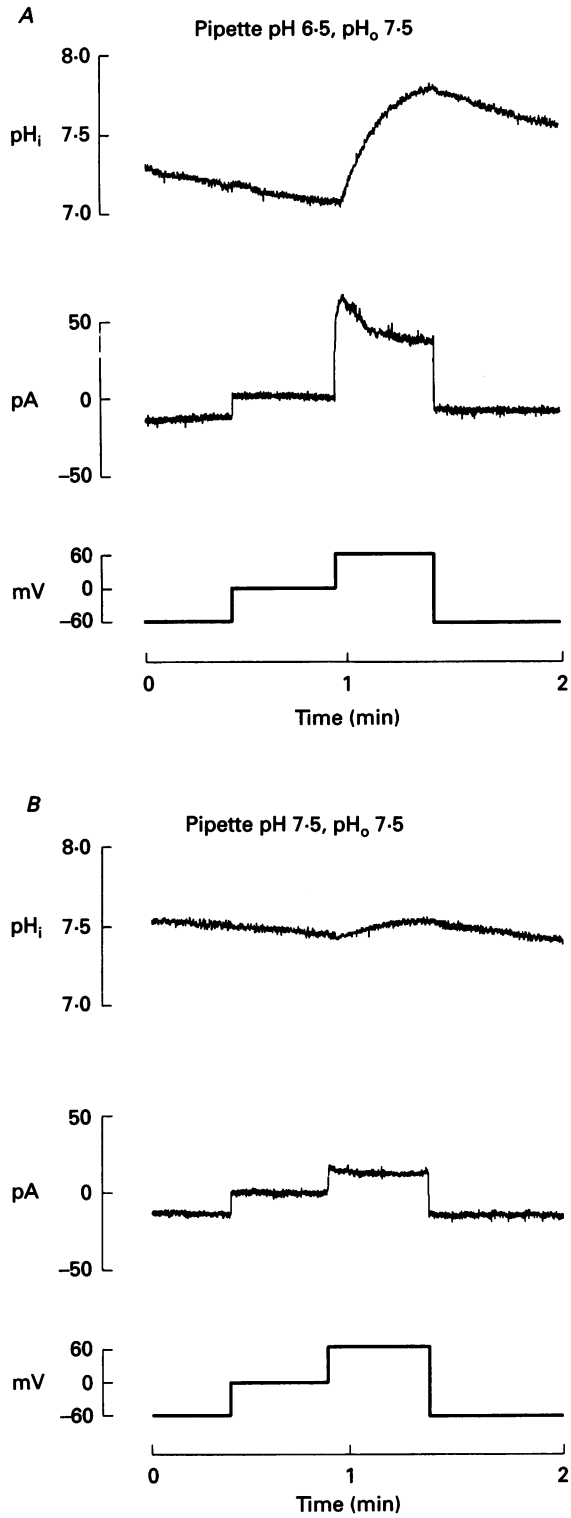

Fig. 2. For legend see facing page.

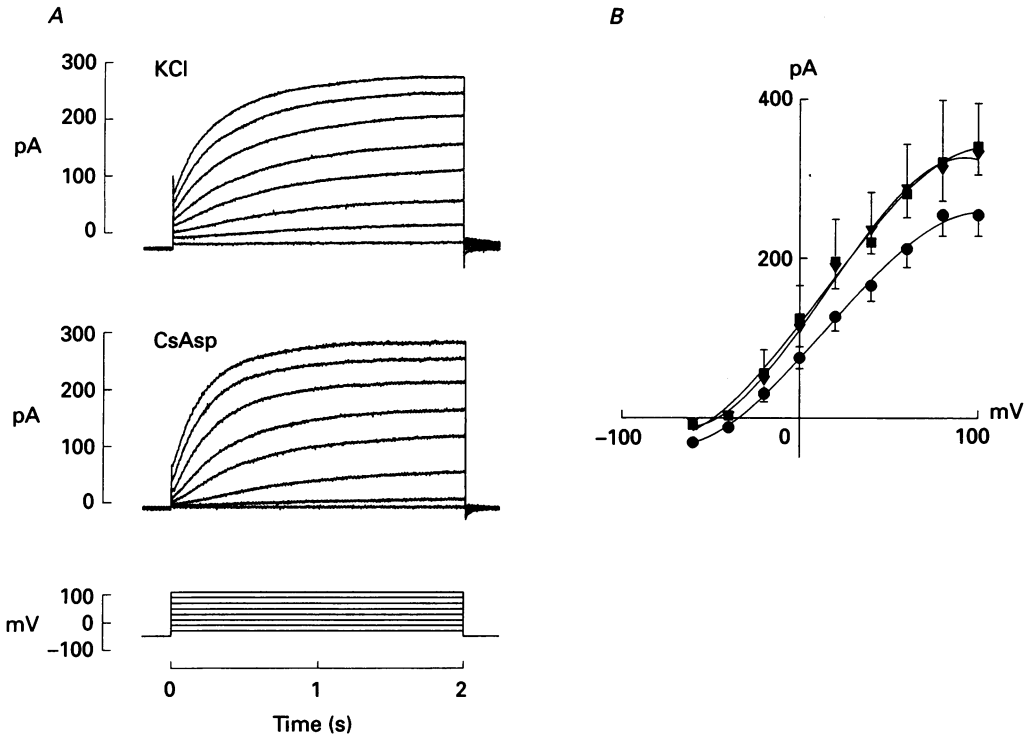

Fig. 3. Effect of ionic substitution on the voltage-activated currents. HL-60 cells were voltage-clamped at −60 mV in the whole-cell configuration and depolarizing pulses lasting 2 s were applied at 10 s intervals in 20 mV increments (*A*, bottom trace). In all cases, bath pH was 7·5 and pipette pH 5·5. *A*, families of whole-cell currents recorded in bilateral KCl (BS II–PS V, upper panel) or CsAsp (BS IV–PS VII, middle panel) solutions. *B*, steady-state current–voltage relationship derived from experiments like those in *A*. Experiments were performed in bilateral KCl (●), NaCl (▼) or CsAsp (■) solutions. Currents were measured at the end of the 2 s depolarizing pulse. Values are means ± S.E.M. of 5 to 8 different cells; the lines through the experimental points were drawn by eye.

A 3×10^8 ions/s flux through a conductive pathway will generate a current of 50 pA. Thus, the magnitude of the observed outward current (Fig. 2*A*) corresponds well to the expected H^+ ion fluxes, suggesting that H^+ efflux through a voltage-activated membrane conductance is responsible for both the measured changes in pH_i and the concomitant outward current. We therefore performed additional experiments to determine if this conductance was selective for H^+ ions.

Fig. 2. Depolarization increases pH_i and activates an outward current. Carboxy-SNARF-1-loaded HL-60 cells were voltage-clamped at −60 mV in the whole-cell configuration. Where indicated, voltage was changed first to 0 mV, then to +60 mV for 30 s. The voltage protocols are shown in the lower traces. The associated currents are depicted in the middle traces and pH_i is shown in the top traces. Bath and pipette contained KCl solutions with low buffering power (10 mM). *A*, pipette pH was 6·5 (solutions PS II; see Table 1). *B*, pipette pH was 7·5 (solutions PS I). The pH of the bath was 7·5 in both cases (solution BS I). Traces are representative of 14 (pH 6·5) and 9 (pH 7·5) experiments.

H^+ selectivity: ion exchange experiment

In the experiments described above, K^+ and Cl^- were the predominant ions in the pipette and bath solutions. To investigate their contribution to the observed currents, we varied their content in the pipette and bath solutions and kept a constant H^+ ion gradient. Pipette solutions with an acidic pH (5·5) were chosen, as

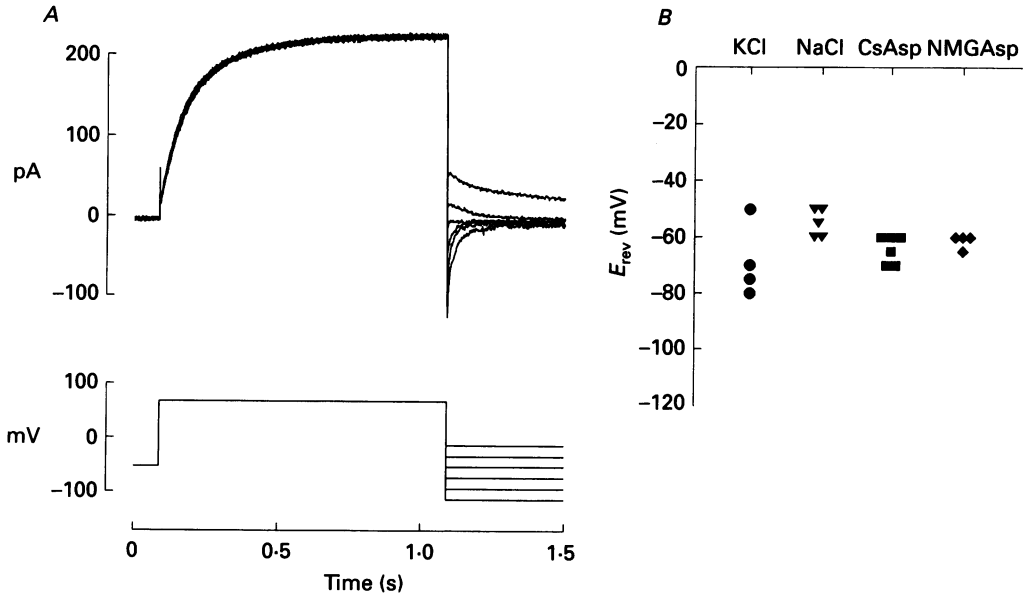

Fig. 4. Reversal potential (E_{rev}) of the tail currents: dependence on K^+, Cl^-, and Na^+. Membrane potential was depolarized to +60 mV for 2 s and then stepped back to test potentials ranging from −120 to −20 mV. The voltage protocol is illustrated in *A*, bottom panel. In all cases, bath pH was 7·5 and pipette pH 5·5. *A*, whole-cell currents elicited by the voltage protocol with NaCl in bath and pipette (solutions BS III and PS VI). In this experiment $E_{rev} = -60$ mV. *B*, comparison of the reversal potentials measured in bilateral KCl (●), NaCl (▼), CsAsp (■), and NMGAsp (◆) solutions. E_K, E_{Na}, E_{Cs}, $E_{NMG} = +3{\cdot}24$ mV; E_{Cl}, $E_{Asp} = +4{\cdot}61$ mV. Points represent determinations of E_{rev} from individual experiments.

a current due to H^+ efflux would be larger at lower pH_i. Media with high buffering power (100 mM Mes) were prepared, to better equilibrate the pipette and cytosolic compartments (see Fig. 1) and to minimize voltage-induced changes in pH_i during the course of the measurements. Experiments were performed in bilateral KCl, NaCl, or caesium aspartate (CsAsp) solution. The cells were held at −60 mV and currents activated by applying 2 s depolarizing pulses ranging from −40 to +100 mV. Under these conditions, outward currents were elicited at voltages > −40 mV, regardless of the ionic composition of the medium (Fig. 3). Activation of the current was relatively slow, reaching half-maximal activation after 200 ms at +60 mV. Full activation of the current was observed within 1–2 s. Comparable results were also obtained using bilateral solutions of *N*-methyl-D-glucammonium aspartate (NMG-Asp; not shown). The prevalence of the outward current under such a variety of ionic conditions could

suggest that the underlying conductance is extremely non-selective, unable to discern between the organic and inorganic substituents used. Alternatively, and more likely (see below), the data may indicate that an ionic species other than the major cationic and anionic constituents of the medium carries the current.

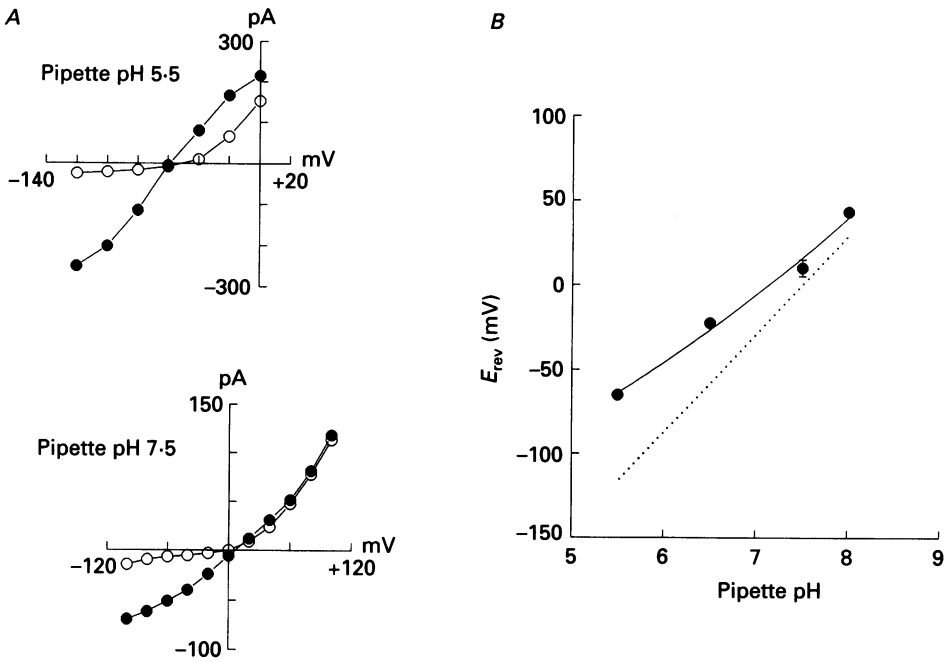

Fig. 5. Reversal potential of the tail currents as a function of pipette pH. Cells were suspended in CsAsp solution, pH 7·5 (BS IV) and pipettes contained CsAsp solutions of varying pH (5·5–8·0; solutions PS VII–X in Table 1). Membrane potential was depolarized to +60 mV (for pipette pH 5·5–6·5) or to +120 mV (for pipette pH 7·5–8·0) for 2 s and then stepped back to various test potentials. *A*, tail current amplitude at different membrane potentials with a pipette pH of 5·5 (top panel) and 7·5 (bottom panel). Tail currents were measured 4 ms (●) or 300 ms (○) after stepping back to the test potential. Data are representative of 5–6 experiments and were not corrected for leak. *B*, reversal potentials measured as in *A* are plotted against the pipette pH. Values are means ± S.E.M. of 5–6 experiments. Where absent, error bar is smaller than symbol. The dotted line represents the E_{rev} calculated assuming that the conductance is perfectly H^+ selective and that the cytosolic pH equilibrates with the pipette pH.

H^+ selectivity: reversal potential of tail currents

The identity of the permeant species was established by analysing the reversal potential of the tail currents, E_{rev}. The conductance was initially activated by application of depolarizing pulses (+60 mV for 2 s). Test pulses between 0 and −100 mV were then imposed and the inactivating currents were recorded (Fig. 4*A*). Under the conditions used (bilateral solutions of the major salt, pipette pH 5·5 and external pH 7·5), the equilibrium potentials of the different ions are: E_K, E_{Na} and $E_{Cs} = +3{\cdot}24$ mV; E_{Cl} and $E_{Asp} = +4{\cdot}61$ mV; $E_H = -116$ mV. As illustrated in Fig.

4*B*, the measured E_{rev} ranged between −50 and −80 mV and was not significantly different when measured in KCl, NaCl, CsAsp or NMG-Asp solutions. These results demonstrate that the reversal potential of the current is largely independent of the presence of the main physiological ions, namely K^+, Na^+ and Cl^-. Instead, the strongly negative E_{rev} is consistent with translocation of H^+ ions through the

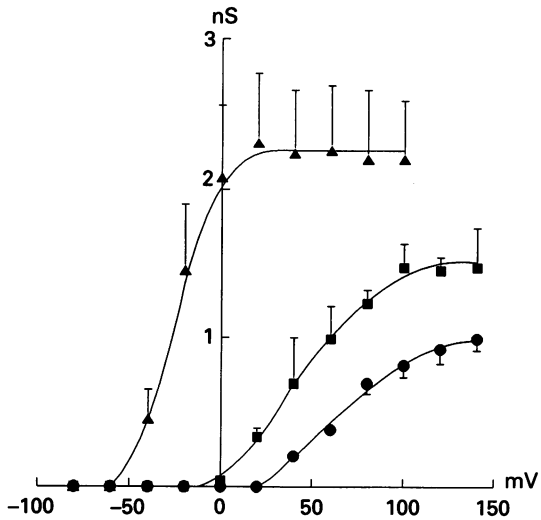

Fig. 6. pH dependence of the H^+ conductance. Cells were suspended in CsAsp solution, pH 7·5 (BS IV) and pipettes contained CsAsp solutions of varying pH (5·5–7·5; solutions PS VII–IX in Table 1). Depolarizing pulses lasting 2 s were applied at 10 s intervals in 20 mV increments from a holding voltage of −60 mV. Currents were measured at the end of the 2 s depolarizing pulse, and the H^+ chord conductance calculated according to eqn (1) in the text. The conductance–voltage relationships measured with a pipette pH of 5·5 (▲), 6·5 (■), and 7·5 (●) are shown. Values are means ± S.E.M. of 5 to 8 different cells; the lines through the experimental points were drawn by eye.

voltage-sensitive conductance. The latter hypothesis is also in accordance with the pH_i changes recorded in Fig. 2.

To confirm the involvement of H^+ ions in the outward current, the pH_i dependence of E_{rev} was determined at a constant extracellular pH of 7·5. Bilateral solutions of the presumed impermeant ions CsAsp were used and different buffering species were utilized to maintain high buffering capacity at the varying levels of pH_i tested (see Table 1 for details). The conductance was activated by depolarizing pulses, and the voltage then stepped back to various test potentials. The current–voltage relationship for the tail current amplitude measured 4 ms after repolarization was linear over the range of voltages tested, regardless of the pipette pH (Fig. 5*A*, ●). However, the current did not deactivate at positive voltages, as assessed by the tail current amplitude measured 300 ms after repolarization (Fig. 5*A*, ○). Therefore, the instantaneous current–voltage relationship could only be determined for negative voltages, where it showed no rectification. As the pipette pH was changed from 5·5 to 8·0, E_{rev} (taken as the intersection of the two plots at 4 and 300 ms) changed from -65 ± 2 to $+43 \pm 3$ mV (Fig. 5*B*). Thus, while independent of the main ionic species, the measured E_{rev} is responsive to the sign and magnitude of the H^+ gradient.

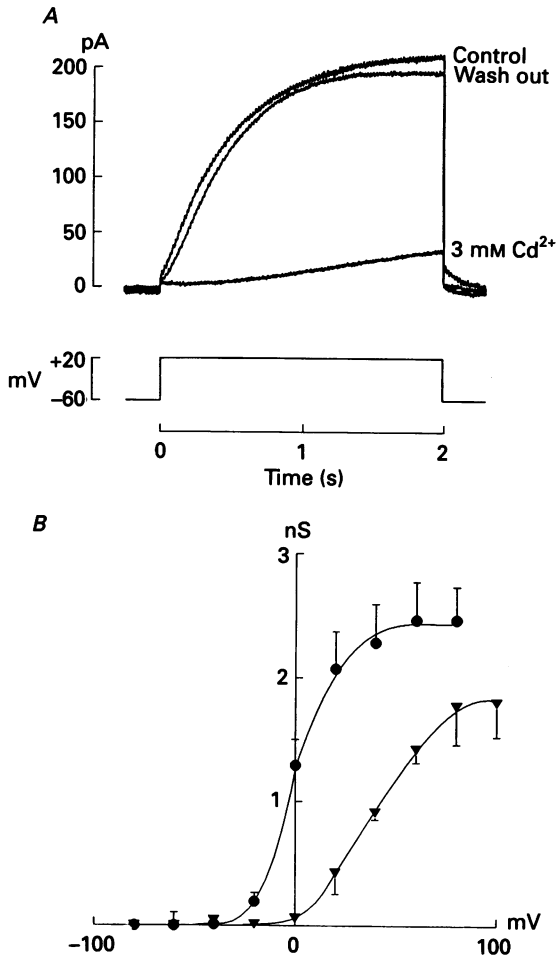

Fig. 7. Effect of external Cd^{2+} ions on the H^+ conductance. Bath and pipette contained CsAsp solutions, bath pH 7·5 (BS IV), pipette pH 5·5 (PS VII). *A*, the current elicited by a depolarization to +20 mV is reversibly blocked by the addition of 3 mM Cd^{2+} to the external solution (corresponding to a free Cd^{2+} concentration of 150 μM). *B*, conductance–voltage relationships measured in the absence (●) and in the presence (▼) of 3 mM Cd^{2+}. Values are means ± S.E.M. of 6 different cells; the lines through the experimental points were drawn by eye.

Together, the data in Figs 2–5 indicate that the voltage-activated outward current is carried primarily, if not entirely, by H^+ ions.

pH sensitivity of the H^+ conductance

At constant voltage, the current amplitude increased with decreasing internal pH, as expected from the increase in the driving force for H^+ (Fig. 2). However, analysis of the conductance–voltage curves measured at different pipette pH showed that a change in pH_i had additional effects on the voltage-activated H^+ conductance (Fig.

6). The whole-cell conductance for H^+, G_H, at different voltages was calculated using the equation:

$$G_H = I_H/(V_m - E_{rev}), \quad (1)$$

where I_H is the measured H^+ current, V_m the membrane potential during the depolarizing pulse, and E_{rev} the measured reversal potential of the H^+ current. Cytosolic acidification both increased the maximal H^+ conductance and shifted the conductance–voltage relationship to more negative voltages. The threshold voltage for the activation of G_H was -60 mV when $pH_i = 5{\cdot}5$, -20 mV when $pH_i = 6{\cdot}5$ and $+20$ mV when $pH_i = 7{\cdot}5$. Thus, acidification renders the H^+ conductance more susceptible to activation by depolarization.

Block by divalent metal cations

Similar to the H^+ conductances described in snail neurons, axolotl oocytes, and rat epithelial cells, the H^+ currents in HL-60 cells were reversibly blocked by divalent cations (Fig. 7). When 3 mM Cd^{2+} was added to the external solution (corresponding to a free Cd^{2+} concentration of 150 μM), three main effects on the H^+ conductance were observed: (1) the maximal conductance was reduced (Fig. 7*B*), (2) the conductance–voltage relationship was shifted to more positive voltages (Fig. 7*B*), and (3) the kinetics of activation were prolonged (not shown). These effects were reversible (Fig. 7*A*). External Cd^{2+} also blocked the depolarization-induced pH_i increase, as measured with SNARF-1 fluorescence (not shown). Similar results were obtained with 3 mM Zn^{2+} (not shown).

DISCUSSION

The increased rate of H^+ production by activated neutrophils has been well documented (Segal, Geisow, Garcia, Harper & Miller, 1981; van Zwieten, Wever, Hamers, Weening & Roos, 1981) and attributed primarily to the NADPH oxidase and the associated acceleration of the hexose monophosphate shunt (Borregaard *et al.* 1984). Less is known about the processes mediating extrusion of the metabolically generated acid from the cells. It is clear that a substantial fraction of the H^+ ions are translocated by the electroneutral Na^+–H^+ antiport (Grinstein & Furuya, 1986). In addition, the existence of a H^+ conductive pathway was inferred from measurements of pH_i while manipulating the membrane potential by means of ionophores (Henderson, Chappell & Jones, 1987; Nanda & Grinstein, 1991; Kapus *et al.* 1992).

Human granulocytes possess a H^+ conductance

In this report, the existence of a H^+ conductance is demonstrated directly, by electrophysiological means. The following findings support the notion that H^+ conductive pathways exist in HL-60 granulocytes: (a) depolarization induced a cytosolic alkalinization in parallel with an outward current of a size corresponding to the expected H^+ ion fluxes (Fig. 2); (b) the outward current persisted after replacement of the major physiological ions with non-permeant substituents (Fig. 3); (c) the reversal potential of the tail currents varied along with the transmembrane

H^+ gradient, but was virtually insensitive to replacement of any of the other ions tested (Fig. 4), and (d) the reversal potential of the tail currents was close, though not equal, to the predicted equilibrium potential for H^+ ions (Fig. 5).

Selectivity of the H^+ currents

The conductance elicited by depolarization in granulocytes is extremely selective for H^+ and would therefore seem ideally suited for regulation of intracellular pH. Relative permeabilities can be roughly estimated from E_{rev}, using the Goldman–Hodgkin–Katz equation. Thus, the deviation of E_{rev} from the calculated H^+ equilibrium potential (~ 50 mV at $pH_i = 5{\cdot}5$ and external pH = 7·5) could be accounted for assuming that the major monovalent cation is approximately one million-fold less permeant than H^+. This is a minimum estimate, as alternative mechanisms may be invoked to explain the deviation of the measured and calculated E_{rev} (see below).

Deviation of E_{rev} from E_H

Three tentative explanations can be offered to account for the deviation of the measured E_{rev} from the predicted H^+ equilibrium potential. First, the cytosolic pH may not be identical to the pH of the pipette filling solution. This is suggested by the slight but significant difference between the fluorescence ratios measured in patched cells and those predicted for completely equilibrated cells by the nigericin calibration (see Methods and Fig. 1). Second, the comparatively large H^+ fluxes elicited by the conditioning pulse used for determination of the tail currents may have changed the pH in the vicinity of the membrane, particularly on the cytosolic side where diffusion is more restricted. Indeed, an increase in overall intracellular pH was detected during depolarizing pulses lasting > 2 s, despite the use of the pipette solutions with a high buffering power. Finally, it is conceivable that ions other than H^+ can permeate through the voltage- and pH-sensitive pathway. As discussed in detail below, the permeability of the H^+-selective conductance to one of the major ions need not be large to account for the observed discrepancy between E_{rev} and the H^+ equilibrium potential. On the other hand, the deviation of E_{rev} was also observed when using NMG-Asp medium. To the extent that these organic ions are thought to be impermeant, the latter explanation seems less likely.

Is the current carried by H^+ ions or by H^+ equivalents?

It is difficult formally to distinguish H^+ currents from OH^- currents. Both ions follow the same electromotive force and are expected to move in opposite directions through a permeant pathway, thus causing similar currents and pH_i changes. Similar to studies in other cellular systems, we have noted that the current saturates at high voltages and that the amplitude at which the current saturates decreases with a decreasing intracellular H^+ ion concentration (not shown). As under these conditions the concentration of external OH^- remains constant while the concentration of internal H^+ is changed; this observation favours the hypothesis that saturation is due to limitation in the supply of H^+ ions by the cytosol. Thus, as discussed elsewhere (Byerly *et al.* 1984; DeCoursey, 1991), the current is probably carried by H^+ rather than by OH^- ions.

Similarities with the other described H^+ currents

H^+ selective currents have been reported in three other cell types: snail neurons (Thomas & Meech, 1982; Byerly *et al.* 1984; Meech & Thomas, 1987), axolotl oocytes (Barish & Baud, 1984) and, more recently, alveolar epithelial cells (DeCoursey, 1991). While the kinetics of activation seems to differ somewhat (< 25 ms in neurons, 300 ms in oocytes and > 1 s in epithelial cells), other properties are remarkably similar in all cell types, including HL-60 granulocytes. These include the steeply rectifying behaviour of the steady-state currents, the increase in conductance and the shift in the threshold for voltage activation caused by intracellular acidification, and the sensitivity to Cd^{2+} and/or Zn^{2+}.

Amplitude of the H^+ currents

It is also noteworthy that the measured currents in HL-60 cells are remarkably large, despite the extremely low concentration of the transported ionic species. When the command voltage was clamped at +60 mV, the steady-state current was in the range of 200–300 pA per cell. This exceeds by a factor of ten the amplitude of the K^+ currents reported in human neutrophils (Krause & Welsh, 1989), which are the major ionic currents described so far in granulocytes. The magnitude of the conductance is also apparent when comparing the H^+ current density in HL-60 cells with that of alveolar epithelial cells (DeCoursey, 1991), the other mammalian cell type reported to express this conductance. When normalized per unit surface area, estimated from the capacitance, the H^+ current density was ~5-fold greater in HL-60 cells than in alveolar epithelial cells (i.e. maximum current density was 133 $\mu A/cm^2$ as compared to 27·3 $\mu A/cm^2$ in alveolar epithelial cells).

Regulation by physiological agonists

Earlier indications of the existence of a H^+ conductance in granulocytes were based on detection of net displacement of acid equivalents in cells subjected to a known proton-motive force (Henderson *et al.* 1988; Nanda & Grinstein, 1991; Henderson & Chappell, 1992). In these experiments, the cells were stimulated with phorbol esters or with arachidonate. It remains to be determined whether the H^+ fluxes observed in phorbol ester and arachidonate-stimulated cells occur through the pH_i-sensitive, voltage-activated conductance reported. In both cases the H^+ fluxes are comparatively large, and susceptible to inhibition by Zn^{2+} and Cd^{2+} (Nanda & Grinstein, 1991; Kapus *et al.* 1992; and this report). Therefore, it is possible that a single molecular entity is involved in both processes, and that stimulation of cells by phorbol esters or arachidonate increases the sensitivity of the H^+ conductance to pH_i and plasma membrane potential. This possibility is currently under investigation.

Role of the H^+ conductance

Regardless of potential additional regulatory mechanisms, the regulation of the H^+ conductance by plasma membrane potential and intracellular pH, described in this paper, appears ideally suited for a role in pH_i regulation during granulocyte activation. The conductance is seemingly closed at negative potentials but opens during depolarization. This feature would ensure that H^+ permeability remains low

prior to stimulation, precluding electrophoretic uptake of acid equivalents, which would compromise pH_i homeostasis in resting cells. The depolarization known to occur upon neutrophil stimulation (Cross & Jones, 1986; Henderson *et al.* 1988; Ellis, Cross & Jones, 1989) would reverse the direction of the proton-motive force and simultaneously open the conductive pathway. The cytosolic acidification, resulting from the NADPH oxidase and hexose phosphate shunt activity, lowers the threshold of activation of the current by the plasma membrane depolarization (see Fig. 6). Together, these features would ensure effective opening of the conductance only when the net H^+ electrochemical gradient points outward, while preventing spontaneous acidification of unstimulated cells.

We thank Antoinette Monod for help with the culture of HL-60 cells, Drs L. Bernheim and S. Rawlings for discussions. These studies were supported by grant No. 32-30161.90 from the Swiss National Foundation. N.D. was supported by the Swiss League Against Rheumatism, the Reuter Foundation, Geneva, and the Clóetta Foundation, Geneva. S.G. is an International Scholar of the Howard Hughes Medical Institute.

REFERENCES

BABIOR, B. M. (1978). Oxygen-dependent microbial killing by phagocytes. *The New England Journal of Medicine* **298**, 721.

BARISH, M. E. & BAUD, C. (1984). A voltage-gated hydrogen ion current in the oocyte membrane of the axolotl, *Ambystoma*. *Journal of Physiology* **352**, 243–263.

BASSNETT, S., REINISCH, L. & BEEBE, D. C. (1990). Intracellular pH measurement using single excitation–dual emission fluorescence ratios. *American Journal of Physiology* **258**, C171–178.

BORREGAARD, N., SCHWARTZ, J. H. & TAUBER, A. I. (1984). Proton secretion by stimulated neutrophils. Significance of hexose monophosphate shunt activity as source of electrons and protons for the respiratory burst. *Journal of Clinical Investigation* **74**, 455–459.

BORREGAARD, N. & TAUBER, A. I. (1984). Subcellular localization of the human neutrophil NADPH oxidase, b-cytochrome and associated flavoprotein. *Journal of Biological Chemistry* **259**, 47–52.

BUCKLER, K. J. & VAUGHAN-JONES, R. D. (1990). Instruments and techniques: application of a new pH-sensitive fluoroprobe (carboxy-SNARF-1) for intracellular pH measurement in small, isolated cells. *Pflügers Archiv* **417**, 234–239.

BYERLY, L., MEECH, R. & MOODY, W. (1984). Rapidly activating hydrogen ion currents in perfused neurones of the snail, *Lymnaea stagnalis*. *Journal of Physiology* **351**, 199–216.

CLARK, R. A. (1990). The human neutrophil respiratory burst oxidase. *Journal of Infectious Diseases* **161**, 1140–1147.

CROSS, A. R. & JONES, O. T. G. (1986). The effect of the inhibitor diphenylene iodonium on the superoxide-generating system of neutrophils. *Biochemical Journal* **237**, 111–116.

DECOURSEY, T. E. (1991). Hydrogen ion currents in rat alveolar epithelial cells. *Biophysical Journal* **60**, 1243–1253.

DEMAUREX, N., SCHLEGEL, W., VARNAI, P., MAYR, G. W., LEW, D. P. & KRAUSE, K. H. (1992). Regulation of Ca^{2+} influx in myeloid cells: role of plasma membrane potential, inositol phosphates, cytosolic free $[Ca^{2+}]$, and filling state of intracellular Ca^{2+} stores. *Journal of Clinical Investigation* **90**, 830–839.

ELLIS, J. A., CROSS, A. R. & JONES, O. T. (1989). Studies on the electron-transfer mechanism of the human neutrophil NADPH oxidase. *Biochemical Journal* **262**, 575–579.

GRINSTEIN, S. & FURUYA, W. (1986). Characterization of the amiloride-sensitive Na^+–H^+ antiport of human neutrophils. *American Journal of Physiology* **250**, C283–291.

GRINSTEIN, S., FURUYA, W. & BIGGAR, W. D. (1986). Cytoplasmic pH regulation in normal and abnormal neutrophils. Role of superoxide generation and Na^+/H^+ exchange. *Journal of Biological Chemistry* **261**, 512–514.

GRINSTEIN, S., FURUYA, W. & ROTSTEIN, O. D. (1988). Intracellular pH regulation in neutrophils: properties and distribution of the Na^+–H^+ antiporter. *Society of General Physiologists Series* **43**, 303–314.

HAMILL, O. P., MARTY, A., NEHER, E., SAKMANN, B. & SIGWORTH, F. (1981). Improved patch-clamp techniques for high-resolution current recording from cells and cell-free membrane patches. *Pflügers Archiv* **391**, 85–100.

HENDERSON, L. M. & CHAPPELL, J. B. (1992). The NADPH-oxidase-associated H^+ channel is opened by arachidonate. *Biochemical Journal* **283**, 171–175.

HENDERSON, L. M., CHAPPELL, J. B. & JONES, O. T. (1987). The superoxide-generating NADPH oxidase of human neutrophils is electrogenic and associated with an H^+ channel. *Biochemical Journal* **246**, 325–329.

HENDERSON, L. M., CHAPPELL, J. B. & JONES, O. T. (1988). Superoxide generation by the electrogenic NADPH oxidase of human neutrophils is limited by the movement of a compensating charge. *Biochemical Journal* **255**, 285–290.

HILLE, B. (1992). In *Ionic Channels of Excitable Membranes*. Sinauer Associates Inc., Sunderland, MA, USA.

KAPUS, A., SZÁSZI, K. & LIGETI, E. (1992). Phorbol 12-myristate 13-acetate activates an electrogenic H^+-conducting pathway in the membrane of neutrophils. *Biochemical Journal* **281**, 697–701.

KRAUSE, K. H. & WELSH, M. J. (1989). Voltage-dependent and Ca^{2+}-activated ion channels in human neutrophils. *Journal of Clinical Investigation* **85**, 491–498.

MARIOT, P., SARTOR, P., AUDIN, J. & DUFY, B. (1991). Intracellular pH in individual pituitary cells: measurement with a dual emission pH indicator. *Life Sciences* **48**, 245–252.

MEECH, R. W. & THOMAS, R. C. (1987). Voltage-dependent intracellular pH in *Helix aspersa* neurones. *Journal of Physiology* **390**, 433–452.

NANDA, A. & GRINSTEIN, S. (1991). Protein kinase C activates an H^+ (equivalent) conductance in the plasma membrane of human neutrophils. *Proceedings of the National Academy of Sciences of the USA* **88**, 10816–10820.

SEGAL, A. W., GEISOW, M., GARCIA, R., HARPER, A. & MILLER, R. (1981). The respiratory burst of phagocytic cells is associated with a rise in vacuolar pH. *Nature* **290**, 406–409.

SHA'AFI, R. I. & MOLSKI, T. F. (1988). Activation of the neutrophil. *Progress in Allergology* **42**, 1–64.

SIMCHOWITZ, L. (1985). Chemotactic factor-induced activation of Na^+/H^+ exchange in human neutrophils. II. Intracellular pH changes. *Journal of Biological Chemistry* **260**, 13248–13255.

THOMAS, R. C. & MEECH, R. W. (1982). Hydrogen ion currents and intracellular pH in depolarized voltage-clamped snail neurones. *Nature* **299**, 826–828.

VAN ZWIETEN, R., WEVER, R., HAMERS, M. N., WEENING, R. S. & ROOS, D. (1981). Extracellular proton release by stimulated neutrophils. *Journal of Clinical Investigation* **68**, 310–313.